

## Article

# Coating of Leather with Dye-Containing Antibacterial and Conducting Polypyrrole

Fahanwi Asabuwa Ngwabebhoh <sup>1</sup>, Oyunchimeg Zandraa <sup>1</sup>, Tomáš Sáha <sup>1</sup>, Jaroslav Stejskal <sup>1,\*</sup>, Dušan Kopecký <sup>2</sup>, Miroslava Trchová <sup>2</sup> and Jiří Pflieger <sup>3</sup>

<sup>1</sup> University Institute, Tomas Bata University in Zlin, 760 01 Zlin, Czech Republic

<sup>2</sup> Central Laboratories, University of Chemistry and Technology, Prague, 166 28 Prague, Czech Republic

<sup>3</sup> Institute of Macromolecular Chemistry, Academy of Sciences of the Czech Republic, 162 06 Prague, Czech Republic

\* Correspondence: stejskal@utb.cz

**Abstract:** In the search for functional organic biomaterials, leather constituted by collagen fibers was coated with a conducting polymer, polypyrrole. The coating was carried out during the oxidation of pyrrole in an aqueous solution of poly(*N*-vinylpyrrolidone) in the presence of five organic dyes: crystal violet, neutral red, methyl orange, acriflavine, and methylene blue. This technique ensures the uniform coating of collagen fibers with polypyrrole and incorporation of organic dyes. The surface morphology was observed with scanning electron microscopy and the transverse profile, reflecting the penetration of the conducting phase into the leather body with optical microscopy. While the polypyrrole coating endows leather with electrical conductivity, organic dyes are expected to affect the polymer morphology and to provide an antibacterial effect. The lowest sheet resistance and antibacterial activity were obtained with crystal violet. This type of coating was characterized in more detail. Infrared spectroscopy confirmed the coating of collagen fibers with polypyrrole and dye incorporation. Mechanical properties were extended to the cyclic bending of the leather at various angles over 5000 cycles. The relative resistance changes were a few percent, indicating good electrical stability during repeated mechanical stress.

**Keywords:** polypyrrole; poly(*N*-vinylpyrrolidone); conducting leather; sheet resistance; bending tests; organic dyes



**Citation:** Ngwabebhoh, F.A.; Zandraa, O.; Sáha, T.; Stejskal, J.; Kopecký, D.; Trchová, M.; Pflieger, J. Coating of Leather with Dye-Containing Antibacterial and Conducting Polypyrrole. *Coatings* **2023**, *13*, 608. <https://doi.org/10.3390/coatings13030608>

Academic Editor: Galina K. Elyashevich

Received: 12 February 2023

Revised: 2 March 2023

Accepted: 9 March 2023

Published: 13 March 2023



**Copyright:** © 2023 by the authors. Licensee MDPI, Basel, Switzerland. This article is an open access article distributed under the terms and conditions of the Creative Commons Attribution (CC BY) license (<https://creativecommons.org/licenses/by/4.0/>).

## 1. Introduction

The use of natural biopolymers in various applications is beneficial because of their ecological production and waste management. It is of obvious concern to endow composites with properties often required by functional materials, such as electrical conductivity or antibacterial performance. Conductivity of organic materials is routinely achieved by coating suitable substrates with conducting polymers, such as polyaniline or polypyrrole. Such composites serve as adsorbents in the dye-pollution treatment of water [1], in electromagnetic interference shielding [2], for corrosion protection of metals [3], as heating elements [4], in supercapacitor electrodes [5], or as decorative leather finishings [6], etc. Antibacterial coatings of materials [7–10] are often required for biomedical applications. Simultaneous conductivity and antimicrobial properties are welcome in electrical monitoring or stimulation of biological objects. One of the strategies to produce conducting polymers with antibacterial properties is outlined below.

Conducting polymers are typically prepared by oxidative polymerization of respective monomers in aqueous media (Figure 1) [11]. The alternative method, electrochemical deposition of conducting polymers, can be applied only to conducting substrates, while the present chemical oxidation of pyrrole is more universal. The reaction is simple, friendly, and easy to control. After the aqueous monomer and oxidant solutions are mixed, the

exothermic polymerization proceeds at room temperature in open air; it is completed in tens of minutes, and the precipitated conducting polymer is separated by filtration. Virtually any surface of the material immersed in the reaction mixture during the oxidative polymerization of pyrrole or aniline becomes coated with a thin polypyrrole or polyaniline overlayer of submicrometer thickness [12,13], even though the polymer film adhesion may differ in individual cases. In addition to conductivity, these polymers display also antibacterial activity [6–10].

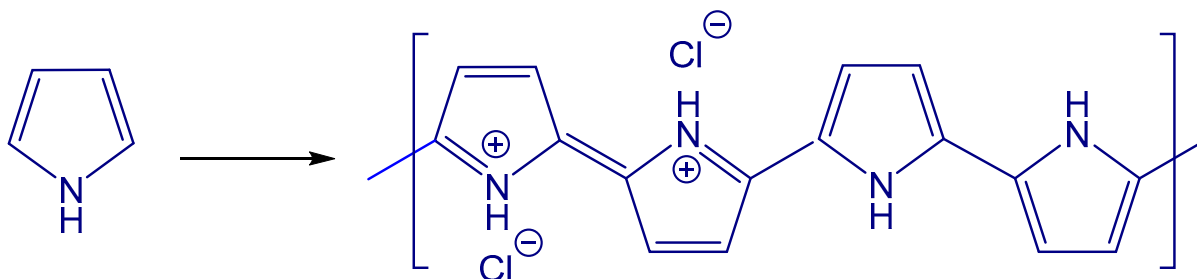


**Figure 1.** Oxidation of pyrrole with iron(III) chloride yields polypyrrole with chloride counter-ions.

Five organic dyes differing in molecular structure have been selected for the present study (Figure 2) for their antibacterial effect reported in the literature: crystal violet (triphenylmethane dye) [14–17], neutral red (phenazine dye) [18,19], methyl orange (azo dye) [20], acriflavine (acridine dye) [21–23], and methylene blue (thiazine dye) [18,22,24].

Antibacterial activity has also been demonstrated in systems including conducting polymers, such as polyaniline [25–27] and polypyrrole [7–9,20,23,28]. In this case, however, such activity may also be caused by residual reactants, low-molecular-weight by-products, polypyrrole counter-ions (Figure 1), and any potential additives.

Conducting polymers and organic dyes share similarities in their molecular structure [11,29]. They both include the conjugated double bonds system that is responsible for the dyes' color and for the green coloration of polyaniline and brown of polypyrrole. They contain aromatic benzene or pyrrole rings. While conducting polymers are polycations, dyes may be both anionic and cationic. Due to these structural features, conducting polymers and dyes interact by electrostatic forces, hydrophobic dispersion forces, hydrogen bonding, and  $\pi$ - $\pi$  interactions of aromatic moieties. Such interactions manifest themselves by the adsorption of dyes on conducting polymers, the effect used for dye removal in water pollution treatment.

In practice, antimicrobial dyes are adsorbed by conducting polymers [29,30] or, probably more efficiently, added directly to the reaction mixture used for the preparation of conducting polymers [11,23]. In the latter case, the interaction between the generated polypyrrole and dyes enhances the conductivity and affects the polymer morphology. The conversion of globular polypyrrole to polypyrrole nanotubes with improved conductivity in the presence of methyl orange is the best known example [31]. Polypyrrole is also preferred to polyaniline in everyday applications due to its reduced sensitivity to pH changes and good conductivity under physiological conditions [32]. For that reason, the leather was coated in the present study with polypyrrole in the presence of organic dyes and the resulting material was tested for conductivity and antibacterial performance.

Leather was selected as a widely exploited biomaterial in footwear production. The conductivity afforded by polypyrrole coatings can be used to produce materials with anti-static properties or to detect mechanical stress. The value-added antimicrobial performance would also be of practical interest.

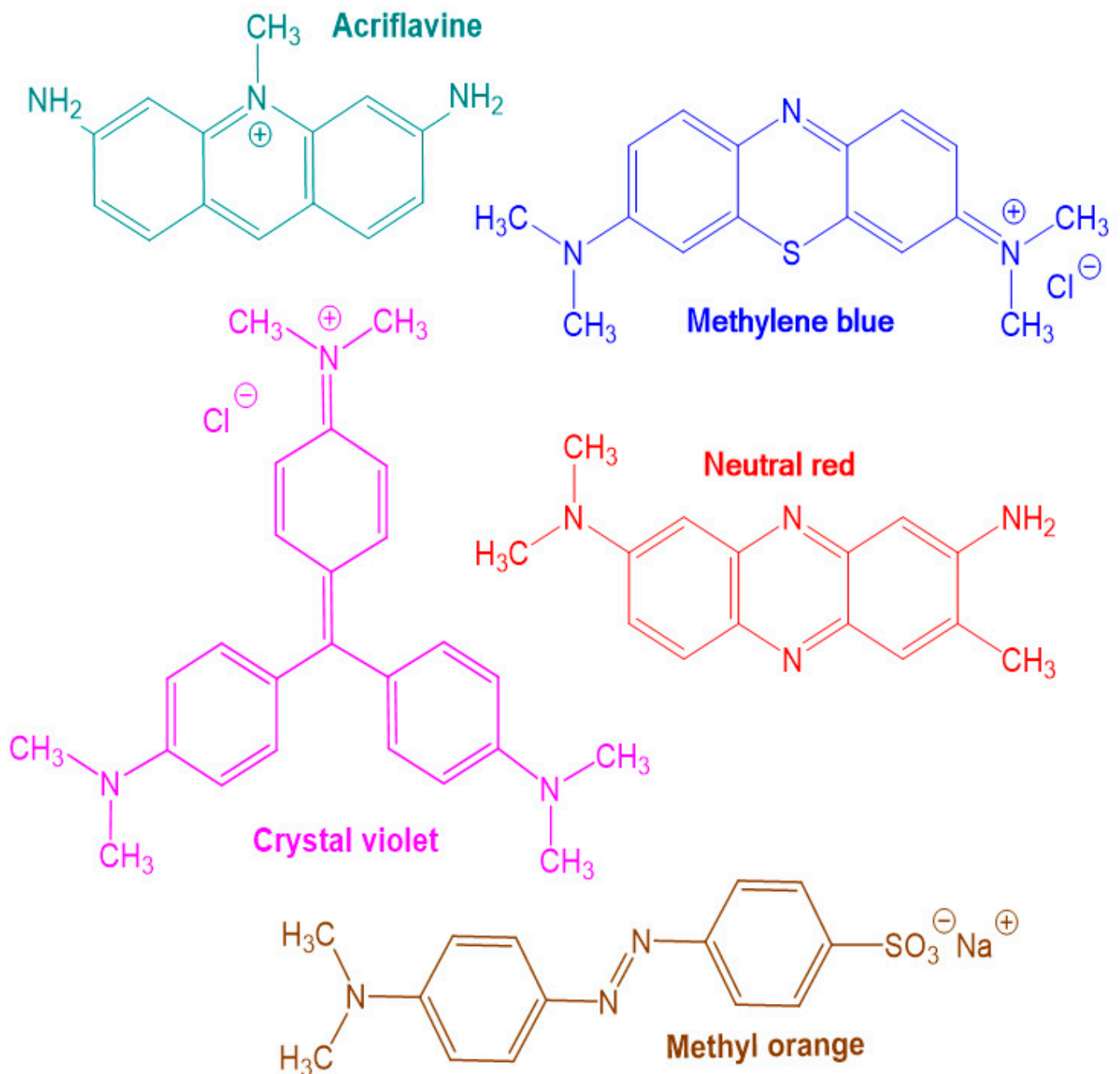


**Figure 2.** Molecular structure of organic dyes: acriflavine, methylene blue, crystal violet, neutral red, and methyl orange.

## 2. Experimental Methods

### 2.1. Materials

The commercial flat-lining chrome-plated pigskin leather known as Velur with an average thickness of 0.8 mm was supplied by the Footwear Research Centre, Tomas Bata University in Zlin, Czech Republic. Pyrrole, iron(III) chloride hexahydrate, hydrochloric acid (37%), ethanol (98%), poly(*N*-vinylpyrrolidone) (PVP; K-90, molecular weight 360,000), and the various organic dyes were supplied by Sigma Aldrich (Prague, Czech Republic). The dyes were used as delivered without any correction for the true dye content specified by the supplier.

## 2.2. Polypyrrole Coating

The pigskin chrome-plated leather was coated with polypyrrole produced via the in situ colloidal dispersion method as previously described with slight modification [6,33,34]. Before the coating process, 100 mL of 0.1 M pyrrole aqueous solution, 4 wt% poly(*N*-vinylpyrrolidone) (PVP), and 0.004 M organic dye were prepared. Then, 100 mL of 0.25 M iron(III) chloride hexahydrate solution was also prepared separately. Both solutions were mixed and the final reaction mixture contained 0.05 M pyrrole, 0.125 M iron chloride hexahydrate (III), 2 wt% PVP, and 0.002 M organic dye. Leathers of dimensions  $15 \times 10 \text{ cm}^2$  immersed in PVP solution were quickly transferred to the freshly prepared reaction mixture and incubated for 1 h to allow for oxidative polymerization of pyrrole to proceed. The presence of PVP prevents the contamination of the leather surface with polypyrrole precipitate produced outside the leather and a colloidal polypyrrole dispersion is generated instead. Once the polypyrrole coating was completed, the leathers were removed and rinsed repeatedly with 0.1 M hydrochloric acid until no colored by-products were released. The last procedure was repeated by immersion in an ethanol bath, followed by drying in open air.

## 2.3. Surface and Bulk Sheet Resistance

The surface and bulk sheet resistances were determined for the polypyrrole-coated substrates using a linear four-probe method with a Jandel cylindrical probe. Current probes were connected to a Keithley 230 power supply (Keithley Instruments, Cleveland, OH, USA), a Keithley 196 multimeter was used as a current source, and potential probes were connected to a Keithley 181 nanovoltmeter for the voltage-drop measurements. The current was reduced to keep the dissipated energy below  $50 \mu\text{W}$ . The Jandel probe was placed at three places within the rectangular inner area that was  $13 \times (17\text{--}35) \text{ mm}^2$  in size. The surface sheet resistance was calculated from the linear part of the I–V characteristics according to the formula  $R_{\text{SR}} = 4.53 \times U/I$ , assuming that the thickness of the conducting layer was much smaller than the distance between the probes. Measurements were made on both sides of the coated leathers in two perpendicular directions at five positions for each direction, and the average values were recorded. Bulk sheet resistance was also measured using the standard two-electrode method. Electrodes were painted with colloidal silver over the edges at opposite sites, and the conductivity over the edge was verified to ensure contact with the inner part of the materials. The sheet resistance was evaluated using a Keithley 617 electrometer. Measurements were made with electrode pairs at two different points and average values were recorded. In general, the bulk resistance is the parallel combination of inner and surface resistance, and it is not possible to distinguish contributions unless they differ markedly. Moreover, the electrode geometry is different in both cases.

## 2.4. Antibacterial Properties

The bacteria species *Staphylococcus aureus* CCM 4516 and *Klebsiella pneumoniae* CCM 4415 strains were obtained from the Czech Republic Centre for Collection of Microorganisms and were used to evaluate the antibacterial activity of the coated leathers. The test was performed according to the ISO 27447 standard for testing of antimicrobial properties of materials and products in the leather industry. The test leather materials were cut into spherical shapes 10 mm in diameter and sterilized. Their antibacterial activity was subsequently evaluated by the agar disc-diffusion method. Bacterial suspensions of each bacteria stock with an approximate concentration of  $9 \times 10^8 \text{ CFU mL}^{-1}$  were inoculated onto the surface of prepared agar plates and the leather samples were placed on the surface followed by incubation for 24 h at  $37 \text{ }^\circ\text{C}$ . The antibacterial activity was then determined by visualization of the agar plates under a (Interscience, Wiesbaden, Germany), to determine the bacteria growth density. The zone of bacterial resistance of the polypyrrole-coated leather was then determined according to the ČSN 79 3380 standard.

### 2.5. Microscopy

Scanning electron micrographs were taken with a Nova NanoSEM electron microscope (FEI, Brno, Czech Republic) to evaluate the surface morphology of the non-coated and coated leathers. Prior to analysis, the leathers were gold sputter coated using a JEOL JFC 1300 Auto Fine coater.

Optical microscopy was used to observe the thickness of coated conductive layers using diffuse light mode and the digital camera of an optical microscope Leica DVM2500 (Leica Microstems, Mannheim, Germany). The light of an incandescent bulb was focused on the samples through a condenser lens and the images were visualized at 100× magnification.

### 2.6. Fourier-Transform Infrared Spectroscopy

FTIR spectra of the leathers were analyzed using a Nicolet 6700 spectrometer (Thermo-Fisher Scientific, Waltham, MA, USA) equipped with reflective ATR extension GladiATR (PIKE Technologies, Fitchburg, WI, USA) with a diamond crystal. The spectra were recorded in the 4000–400  $\text{cm}^{-1}$  range with a deuterated L-alanine-doped triglycine sulfate detector at a resolution of 4  $\text{cm}^{-1}$ , with 64 scans and Happ–Genzel apodization.

### 2.7. Mechanical Properties

The test was carried out according to the ISO 3376 standard using a tensile Instron 5567 (Instron, Norwood, MA, USA) with a static load cell of 3 kN and a crosshead speed of 20  $\text{mm min}^{-1}$  at room temperature ( $\approx 25^\circ\text{C}$ ). Before testing, five test pieces were cut according to ISO 2419 and their width was measured to the nearest 0.1 mm at three positions using a Vernier scale. The thickness of each test piece was also measured as specified by the ISO 2589 protocol at three different positions, and the average value was recorded. The clamp jaws of the tensile testing apparatus were set at 50 mm and a pre-test was performed to determine the maximum force. The tensile strength, Young's modulus, and elongation at break were recorded.

### 2.8. Cyclic Bending

The leather samples were repeatedly bent at a defined angle ( $15^\circ$ ,  $30^\circ$ , and  $45^\circ$ ) on a purpose-made apparatus to test their electromechanical properties [10]. The range of the bending apparatus was from  $-60^\circ$  to  $60^\circ$  with a resolution of  $1^\circ$ . The torque of the servomotor was 11  $\text{kg cm}^{-1}$ , which is, however, counterbalanced by the stiffness of the cantilever. Therefore, the bending angle is relevant only for measurement. The resistivity values were continuously acquired using a PC during 5000 cycles (each cycle lasted 20 s; test > 27 h in total) and from the resistance values in steady state (non-bent  $R_{\text{OFF}}$  and bent  $R_{\text{ON}}$ ) of a relative resistance of the  $n$ -th cycle was calculated as  $|R_{\text{rel}(n)}| = [(R_{\text{ON}(n)} - R_{\text{OFF}(n)})/R_{\text{OFF}(n)}] \times 100$ .

## 3. Results and Discussion

### 3.1. Leather Coating with Polypyrrole

The polymerization of pyrrole via oxidation in an aqueous medium to produce polypyrrole was performed. The leather in contact with the aqueous reaction mixture, i.e., individual collagen fibers, was coated with a thin submicrometer layer of polypyrrole. The coating manifests itself to the naked eye as a change in color (Figure 3). In the absence of any additive, a globular polypyrrole precipitate is formed in the aqueous solution surrounding the leather. Its particles adhere to the coated surface, and they are easily mechanically separated after drying and will contaminate any object in contact. This was prevented by the introduction of a water-soluble polymer, poly(*N*-vinylpyrrolidone). In its presence, colloidal polypyrrole dispersion particles [34] of submicrometer sizes stabilized by PVP outside the leather are produced instead of a polypyrrole precipitate and they are easily removed during the subsequent rinsing with an acid solution. The thickness of the coating on the leather threads becomes more smooth and thinner at the same time.



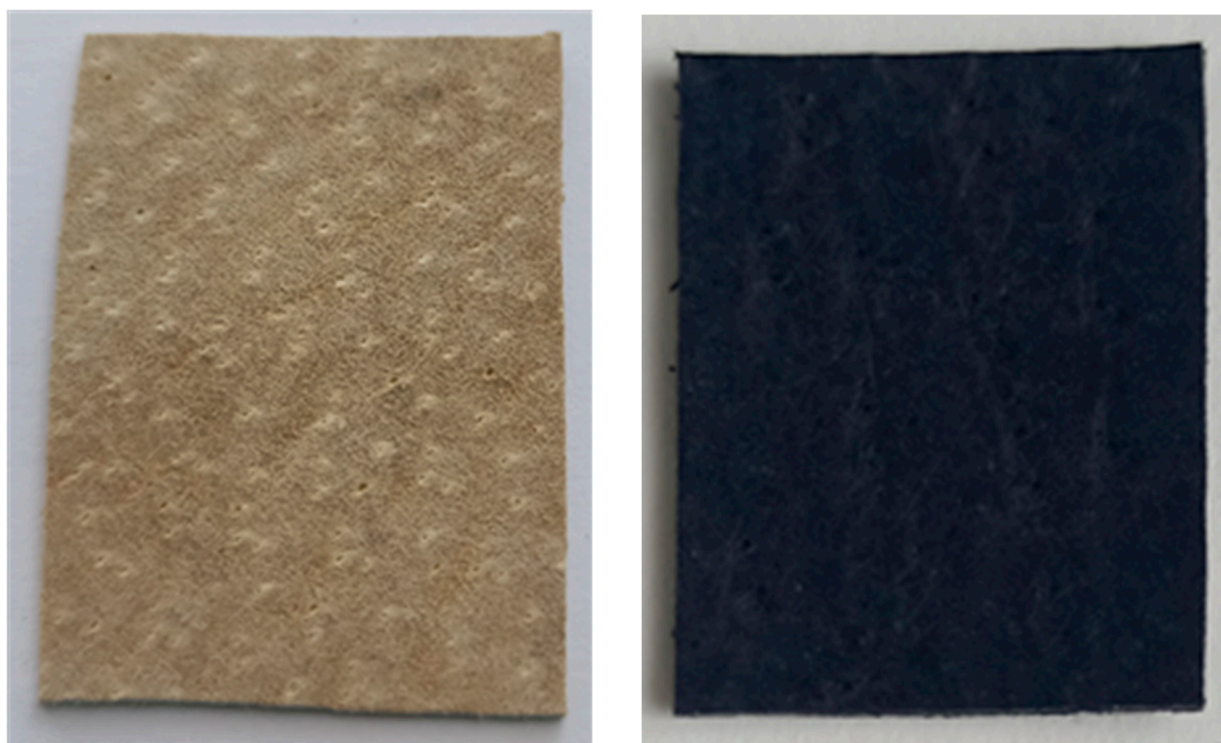


**Figure 3.** Front of the original leather (**left**) and leather coated with polypyrrole in the presence of PVP and crystal violet dye (**right**).

The situation becomes more complex when organic dyes are added to the reaction mixture in order to endow the polypyrrole coating with antibacterial properties. The water-soluble organic dyes play a dual role. First, they act as ionic surfactants because they consist of a large hydrophobic moiety and a hydrophilic cationic or anionic group (Figure 2). Thus, the dye may affect the distribution of reactants in the reaction mixture and the adhesion of intermediates to the leather surface. The second effect is based on the observation that they affect both the morphology and conductivity of polypyrrole [11]. For example, the conversion of globular polypyrrole to polypyrrole nanotubes in the presence of methyl orange in the reaction mixture has been well documented [31].

### 3.2. Surface Morphology

Scanning electron micrographs reveal the fibrous collagen structure of the leathers (Figure 4). The polypyrrole coating of the fibers was thin and smooth, and no contamination by free polypyrrole precipitate was observed. The front of the leather was macroscopically smoother than the reverse side as a result of the surface finish. The fibrous character was clearly visible on both surfaces.

### 3.3. Optical Microscopy

It is necessary to distinguish between the coating of individual collagen fibers and the leather body constituted by many fibers. Although the coating of individual collagen fibers was uniform, the macroscopic distribution of the conducting polymer phase within the leather body was uneven. The thickness of dark conducting layers composed of collagen fibers with deposited polypyrrole was determined by the penetration of the reaction mixture into the leather structure within the time of pyrrole polymerization, which was approximately 10–20 min. The thickness of the dark conducting phase was determined by cross-sectional optical imaging (Figure 5). A significant difference between the front ( $103 \pm 9 \mu\text{m}$ ), and reverse ( $165 \pm 8 \mu\text{m}$ ) sides was observed, which may be attributed to the polished and rougher surfaces. The front and reverse conducting layers were not completely

separated, and in some places they were electrically short-cut. In general, the thickness of polypyrrole deposition was predetermined by the leather hydrophilicity and macroporosity and consequent penetrability of the reaction mixture into its inner structure. The depth of penetration could be varied by decreasing or increasing reactant concentrations or temperature and consequent slowdown or acceleration of the polymerization rate. The increase in the concentration of PVP associated with the increase in viscosity would decrease the extent of penetration. The irregularities observed on the surfaces can be explained by the roughness of the leather (Figure 3), which depends on the leather finishing.

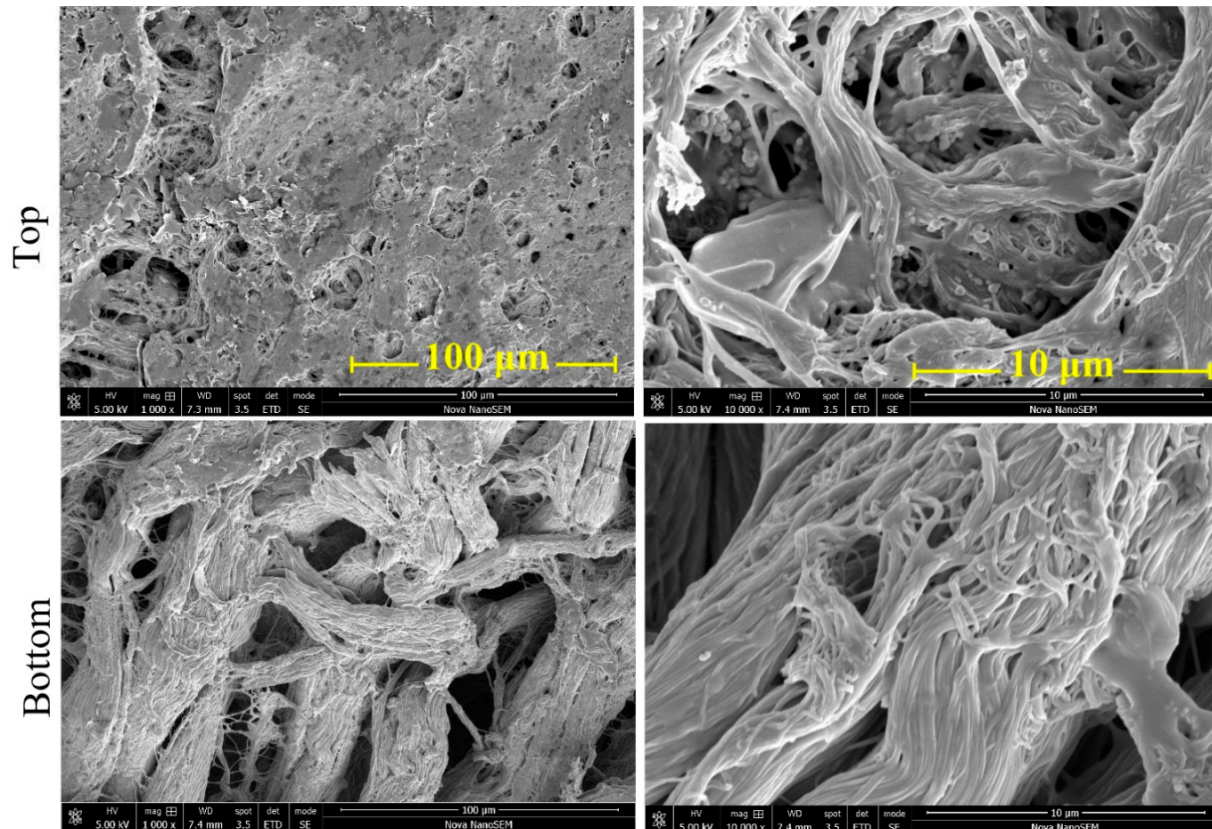


**Figure 4.** Surface morphology of leather coated with polypyrrole in the presence of PVP observed at two magnifications.

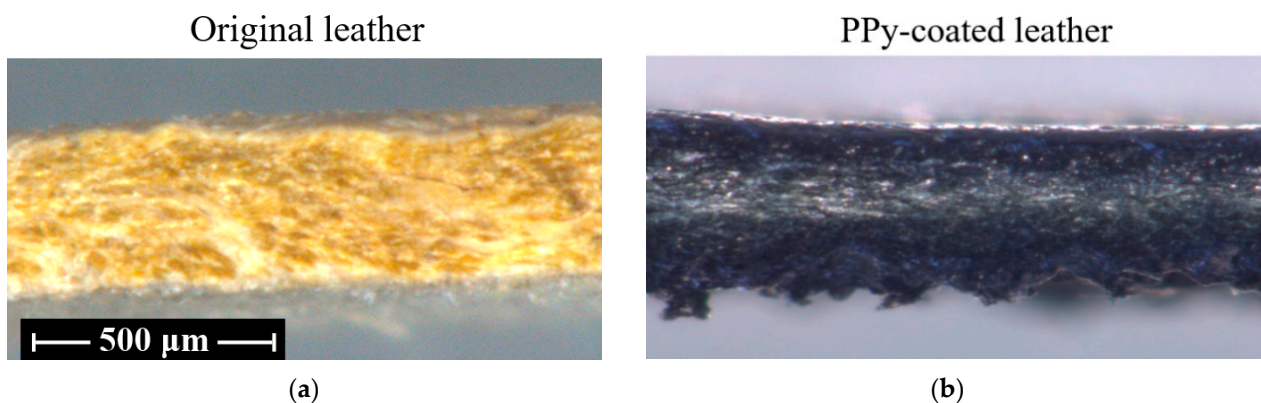


**Figure 5.** Cross-sectional optical microscopic images of (a) leather before and (b) after coating with polypyrrole in the presence of PVP and crystal violet.

### 3.4. Sheet Resistance

Conductivity is the most important parameter in this study. The electrical properties of polypyrrole deposited on similar materials, such as melamine sponges, and their use as pressure-sensitive materials has recently been reported [33,34]. The neat leather did not display any measurable conductivity. After coating with polypyrrole, the surface sheet resistance of the leather material on both sides was in the range of tens of  $k\Omega/sq$  (Table 1). As observed in the literature [34], the deposited polypyrrole overlayer was thinner, i.e., the content of polypyrrole was lower, and sheet resistance increased accordingly by one order of magnitude.

**Table 1.** Sheet and bulk resistances of leather coated with polypyrrole (PPy) in the presence of PVP and organic dyes.

Coating Conditions	Sheet Resistance ( $k\Omega/sq$ )				Bulk Resistance $k\Omega$
	Front		Reverse		
	Horizontal	Vertical	Horizontal	Vertical	
PPy (No PVP)	$7.0 \pm 0.8$		$5.1 \pm 0.2$		n/a
PPy + PVP	$302 \pm 20$		$48 \pm 12$		n/a
PPy + PVP + crystal violet	$0.89 \pm 0.50$	$1.1 \pm 0.1$	$3.4 \pm 0.5$	$0.68 \pm 0.55$	$5.2 \pm 0.4$
PPy + PVP + neutral red	$540 \pm 50$	$470 \pm 130$	$320 \pm 70$	$300 \pm 50$	$60 \pm 10$
PPy + PVP + methyl orange	$3800 \pm 2200$	$3700 \pm 700$	$>10^4$	$>10^4$	$3000 \pm 100$
PPy + PVP + acriflavine	$>10^5$	$>10^5$	$>10^5$	$>10^5$	$>10^5$
PPy + PVP + methylene blue	$>10^5$	$>10^5$	$>10^5$	$>10^5$	$>10^5$

The introduction of organic dyes altered the course of pyrrole formation and deposition in an unpredictable manner. While crystal violet dramatically improved electrical conduction and reduced sheet resistance to units of  $k\Omega/sq$ , neutral red and methyl orange performed less efficiently and the presence of acriflavine and methylene blue led to non-conducting surfaces (Table 1). It has earlier been established that the morphology and conductivity of polypyrrole is affected by the presence of organic dyes in the reaction mixture [11]. It is thus likely that the deposition of polypyrrole will be also influenced in a similar way, which still needs to be investigated. The resistance varied somewhat when measured in horizontal versus vertical directions within one order of magnitude due to the anisotropy and orientation of the leather during processing (Figure 3).

When measurable sheet resistance was found, transverse bulk resistance could also be determined (Table 1). As mentioned above, the front and reverse polypyrrole layers were not perfectly separated (Figure 5) and the occasional short-cuts due to the reaction mixture leaks were responsible for the occurrence of non-zero bulk resistance.

It should be noted that the introductory test of the polypyrrole coating was performed along with other pigskin leathers, the results differed substantially, and the obvious reasons for this could not be identified. The results obtained with the leather used in the present study were the best.

### 3.5. Antibacterial Activity

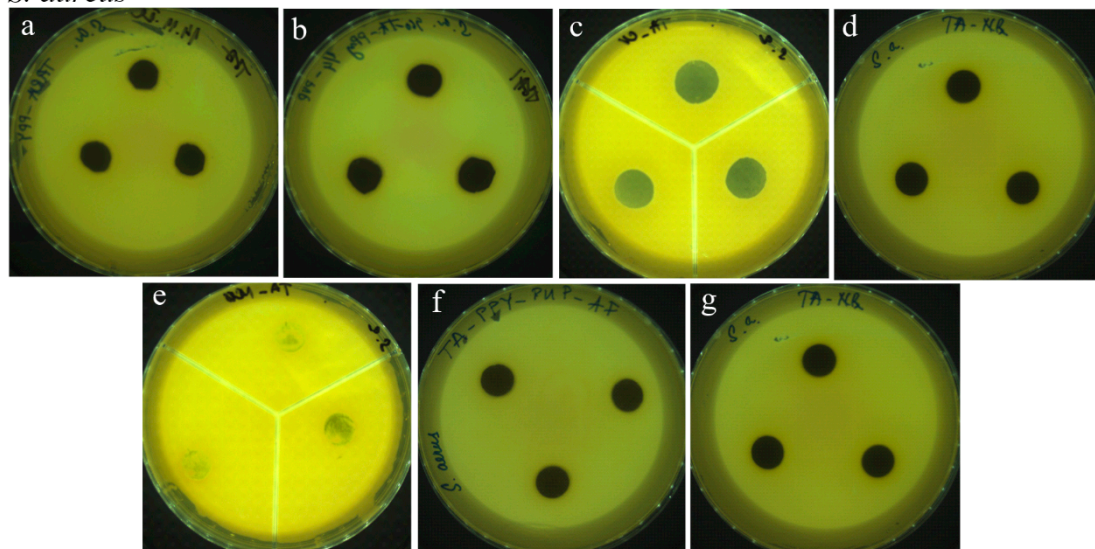
In recent years, antibacterial performance of materials modified with conducting polymers, viz. polypyrrole, has been a subject of scientific interest due to their efficacy in reducing the growth of different bacteria strains [8,9]. Polypyrrole alone has often been reported to display antimicrobial activity [7,23,28–38].

The results of the agar disk-diffusion method [39] applied to bacteria did not show an inhibition zone for the leathers coated with polypyrrole, except for the sample prepared in the presence of crystal violet with an inhibition zone of  $4.3 \pm 1.3$  mm (Figure 6). This method reflects, however, the antibacterial activity of the water-soluble compounds leached from the tested sample. Polypyrrole is insoluble in water, and any positive antibacterial response in this method can be associated only with the residual reactants and by-products



left from the synthesis, counter ions released from polypyrrole due to neutral media [36], and any loosely adsorbed additives [38]. The antibacterial activity reported in the literature for polypyrrole has been interpreted as an electrostatic interaction between this polycation and the negatively charged wall of the bacterial cell [8]. The physical adsorption of bacteria at the polypyrrole surface is followed by the penetration of counter ions that stimulate cell apoptosis. For that reason, the surface morphology is also of importance [38]. The ability of polypyrrole to promote the photocatalytic generation of active oxygen species [29] could also be considered as a supporting mechanism for antibacterial performance.

### *S. aureus*



### *K. pneumoniae*

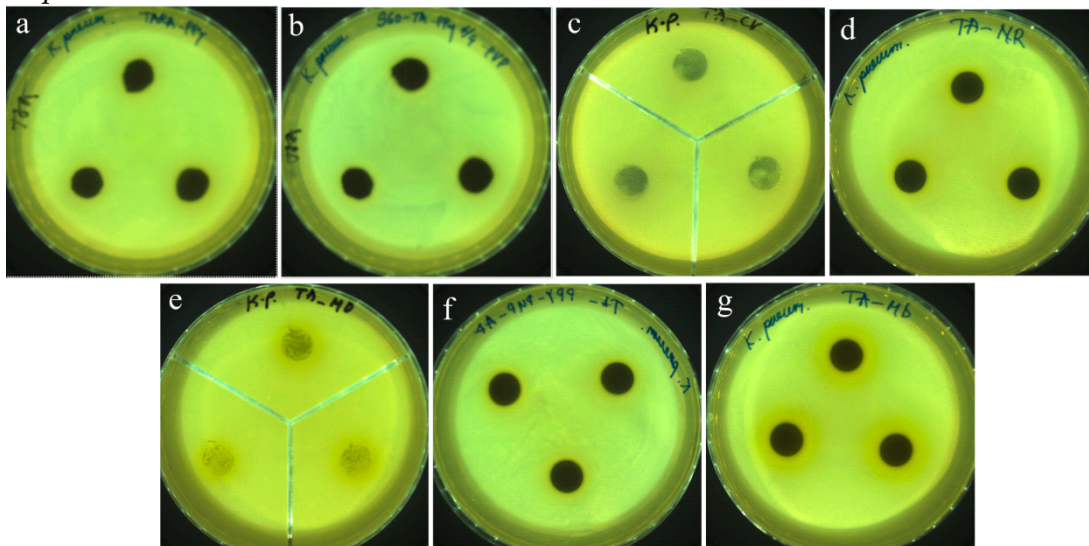


**Figure 6.** Images of inoculated agar plates after 24 h with coated leather materials with (a) polypyrrole, (b) polypyrrole–PVP, and polypyrrole–PVP in the presence of (c) crystal violet, (d) neutral red, (e) methyl orange, (f) acriflavine, and (g) methylene blue in the testing of the antibacterial effect on bacterial strains of *Staphylococcus aureus* (**upper part**) and *Klebsiella pneumoniae* (**lower part**).

The zone of bacterial resistance of the polypyrrole-coated leather was then determined (Table 2). If bacteria do not grow on the surface of a leather test specimen, it means that the material has a sufficient antibacterial effect. A leather for which the bacterial resistance, i.e., the surface without any bacterial growth, is between 75 and 100%, exhibits a positive antibacterial effect. Values between 60 and 75% indicate that the antibacterial

effect is moderate, and less than 60% indicates that there is no antibacterial effect [40]. The antibacterial effect in terms of the zone of resistance was found for all polypyrrole-coated leathers (Table 2), except for leather coated in the presence of methyl orange, which showed resistance below 60%. Methyl orange is not a dye with typical antibacterial activity but it has a special role in the chemistry of polypyrrole, as it guides the formation of polypyrrole nanotubes [11,31]. For that reason, it was included into the present study. In general, the resistance against *S. aureus* was more significant compared to *K. pneumoniae*. This result can be attributed to the cell wall of the Gram-positive bacteria *S. aureus* that contains a thicker layer of peptidoglycans, which is simpler than the Gram-negative wall of *K. pneumoniae*, possessing an additional outer membrane with lipopolysaccharides. This may prevent the interaction of bacteria with the polypyrrole coating present on the surface of collagen fibers in the leather [7,41].

**Table 2.** Zone of bacterial resistance without any bacterial growth (%) on leather coated with polypyrrole in the presence of poly(*N*-vinylpyrrolidone) and organic dyes.

Coating Conditions	<i>Staphylococcus Aureus</i>	<i>Klebsiella Pneumoniae</i>
PPy only, no PVP	100	100
PPy + PVP	100	100
PPy + PVP+ crystal violet	100	60–75
PPy + PVP+ neutral red	100	100
PPy + PVP + methyl orange	<60	<60
PPy + PVP + acriflavine	100	100
PPy + PVP + methylene blue	100	100

The results suggest that polypyrrole alone is able to prevent bacterial growth and the incorporation of organic dyes may only have a supporting role. Because polypyrrole deposition in the presence of crystal violet performed the best with respect to electrical properties, more detailed characterization only for this case is reported below.

### 3.6. FTIR Spectra

The coating of collagen fibers with polypyrrole was studied with ATR FTIR spectroscopy. In the infrared spectra of the front and reverse sides of the leather coated with polypyrrole (spectra L + PPy in Figure 7), we detected bands at  $1732\text{ cm}^{-1}$  (C=O stretching vibrations),  $1657/1632\text{ cm}^{-1}$  (Amide I),  $1547\text{ cm}^{-1}$  (Amide II),  $1238$ ,  $1169$ , and  $1030\text{ cm}^{-1}$ , which belong to the polypeptide chains of the collagen structure of the leather (spectra L in Figure 7) [10]. In addition, we also detect bands of polypyrrole with maxima partially overlying the leather bands located at  $1542\text{ cm}^{-1}$  (C–C stretching vibrations in the pyrrole ring),  $1447\text{ cm}^{-1}$  (C–N stretching vibrations in the ring),  $1284\text{ cm}^{-1}$  (C–H or C–N in-plane deformation modes),  $1163\text{ cm}^{-1}$  (breathing vibrations of the pyrrole rings),  $1030\text{ cm}^{-1}$  (C–H and N–H in-plane deformation vibrations), and  $965$  and  $885\text{ cm}^{-1}$  (C–H out-of-plane deformation vibrations of the ring) [25]. The observation of both collagen and polypyrrole in the spectra means that the conducting coating is thinner than the penetration depth of a few micrometers of infrared radiation. When crystal violet was present in the reaction mixture, we also detected small peaks at  $1583$  and  $1360\text{ cm}^{-1}$  that could be associated with the presence of this dye (spectrum L + PPy + CV in Figure 7).

### 3.7. Mechanical Properties

Mechanical properties of leather represented by the stress–strain dependences are important for practical applications. A load force of 44 N was required to tear the original leather (Table 3). After coating with polypyrrole, the break load force needed for tearing decreased by approximately 30%. The elongation at break was significantly increased as a result of oxidation and/or hydrolytic changes of the collagen fibers by iron(III) chloride. This may have increased the flexibility of the coated leather. The Young’s modulus reflects the stress–strain ratio. After polypyrrole coating, this modulus decreased by approximately

40%. This again indicated that the polypyrrole coating introduced structural changes in the surface morphology of the collagen fibers.

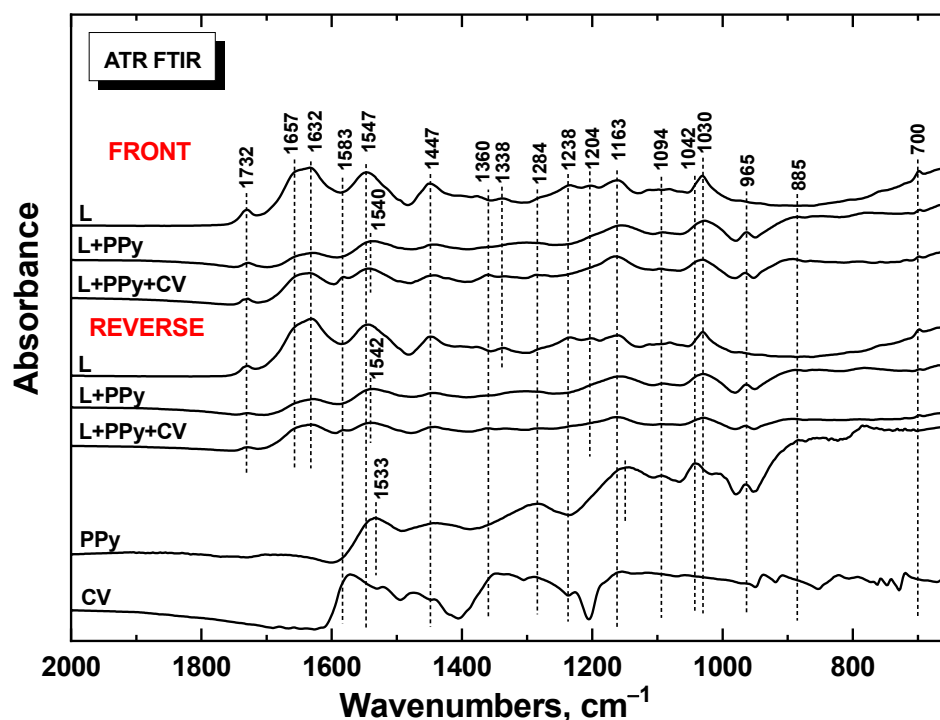


**Figure 7.** ATR FTIR spectra of original (L) and polypyrrole-coated leather (L + PPy) in the absence or presence of crystal violet (CV) recorded from the front and reverse sides.

**Table 3.** Mechanical properties of the original leather and the leather coated with polypyrrole in the presence of poly(*N*-vinylpyrrolidone) and crystal violet.

Leather	Tensile Strength (MPa)	Elongation at Break (%)	Break Load Force (N)	Young's Modulus (MPa)
Original	15.4 ± 0.9	33.5 ± 1.1	43.8 ± 2.7	39.3 ± 1.0
Polypyrrole-coated	9.0 ± 2.3	50.4 ± 4.7	30.7 ± 7.8	23.7 ± 2.1

### 3.8. Cyclic Bending Tests

It is well-known from previous experiments on the synthesis of polypyrrole in the presence of dyes that addition of an auxiliary dye to the in situ polymerization solution may force polypyrrole to create nanostructured morphology and hence to increase its conductivity. However, the excessive amount of dye or residuals of the dye has a negative effect, decreasing overall polypyrrole conductivity [42]. For leathers coated with polypyrrole synthesized in the presence of PVP and various dyes, all samples exhibited higher horizontal sheet resistance (see Table 1) due to the lower conductivity of polypyrrole, compared to the leather sample coated with polypyrrole only. The only exception was the leather sample with polypyrrole deposited in the presence of PVP and crystal violet, whose resistance was lower. Hence, cyclic bending tests were performed, namely, on the sample denoted as PPy + PVP + CV.

The cyclical bending of the leather PPy + PVP + CV led to several interesting observations (Figure 8). First, electrical resistance of all samples was stabilized during the starting ca. 2.5 h of cyclic bending. This phenomenon is probably connected with non-reversible mechanical changes in the structure of the leather (leather softening), which leads to partial interruption of conducting pathways. As a result, the higher the angle of bending, the more intensive is the softening, and the electrical resistance after 2.5 h settled at a new,

higher level. This phenomenon was observed on both sides, i.e., on the finished front and non-finished reverse side. Second, there was an observable difference in the magnitude of electrical resistance between the finished and non-finished sides. The non-finished side had ca. 2–3-fold higher electrical resistance compared to the finished side. Again, this is consistent with the results of the sheet resistance measurements (Table 1). Third, after the initial leather softening, the electrical resistance of the bent leather was relatively stable even after 5000 cycles (>27 h of bending) in the case of the finished side of the leather samples. Fourth, there was a difference in behavior of the non-finished side of the leather after initial softening. The electrical resistance of the non-finished side of the leather fluctuated wildly with mechanical stress, which was easily observable based on the relative resistances calculated for each cycle. The reason for this behavior is probably the structure of unfinished leather that is not flat, but rather “furry”, and composed of thin loose fibers. Hence, the structure of the non-finished side adds randomness to the mechanical and resulting electrical behavior. Still, the long-term resistivity of the non-finished side was relatively stable.

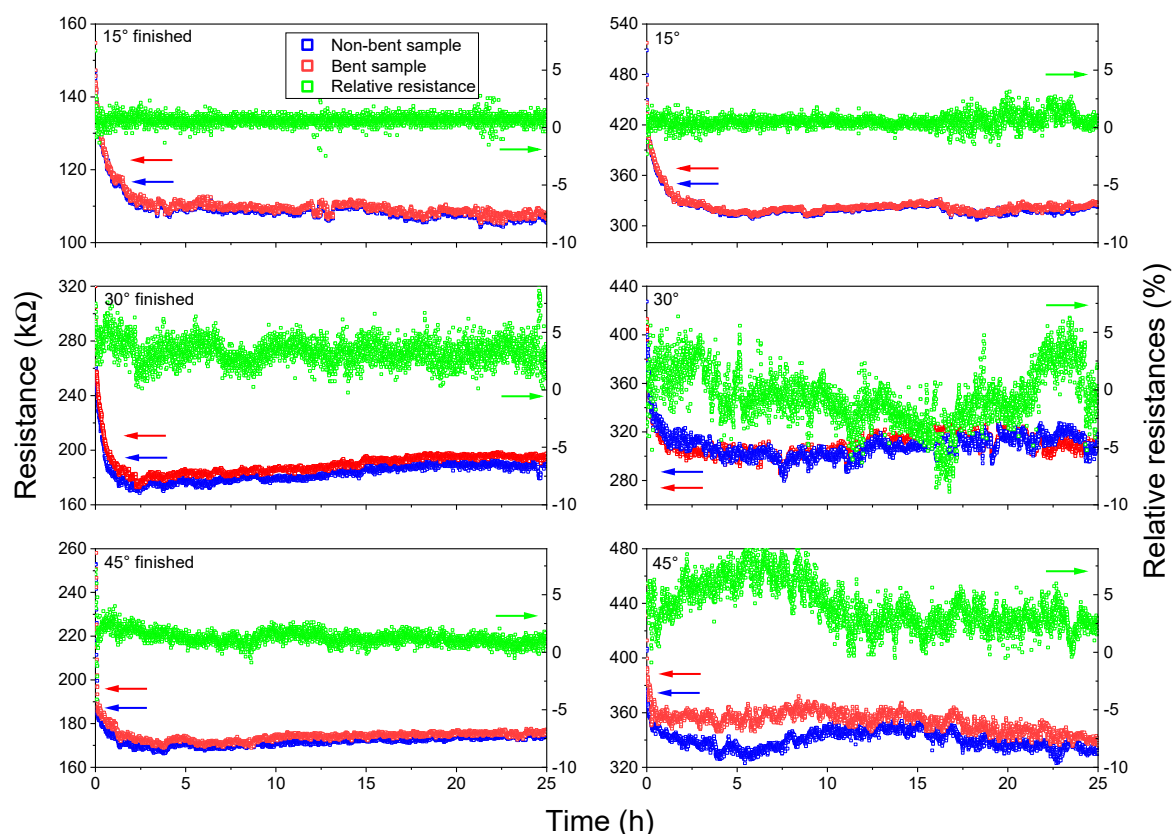


**Figure 8.** Cyclic bending of the leathers coated by polypyrrole synthesized in presence of PVP and crystal violet. Time dependence of resistance measured during 5000 cycles on finished (left) and non-finished, i.e., reverse, (right) sides at angles 15° (top), 30° (middle), and 45° (bottom). Original position (blue), bent sample (red), and relative resistances (green).

#### 4. Conclusions

The leather was made conductive by the deposition of polypyrrole. The dispersion mode of pyrrole polymerization in the presence of poly(*N*-vinylpyrrolidone) provided a submicrometer, smooth coating of collagen fibers constituting the surface layer of the leather structure of ca. 100  $\mu\text{m}$  thickness. The introduction of organic dyes as additives was expected to affect the surface morphology, conductivity and antibacterial performance of coatings. The sheet resistivity after polypyrrole coating in  $\text{k}\Omega/\text{sq}$  increased by two orders of magnitude when the reaction mixture contained crystal violet. Other organic dyes



(neutral red and methyl orange), on the contrary, increased sheet resistance or, in the case of acriflavine and methylene blue, resulted in virtually non-conducting surfaces. The dyes used in the study are known for their antimicrobial activities. The observation of materials exposed to bacterial strains indicates that they are resistant to the contamination of their surfaces by growing bacterial colonies.

The leather modified with polypyrrole in the presence of crystal violet was thus the best conducting and was investigated in more detail. FTIR spectra reveal the presence of the dye in the polypyrrole coating of the collagen fibers. At the same time, such leather displayed an antibacterial behavior that is welcome in the production of special functional footwear. The mechanical properties suggest that some softening of the leather occurred, probably due to hydrolytic changes in the collagen fibers caused by the acidic reaction mixture used for the deposition of polypyrrole. The sheet resistance changed within a few percent after 5000 cycles of bending at various angles.

**Author Contributions:** F.A.N.: methodology, data curation, formal analysis, writing—original draft. O.Z.: formal analysis, data curation. T.S.: supervision, funding acquisition. J.S.: conceptualization, data curation, supervision, writing—original draft. M.T.: methodology, investigation, writing—review and editing. D.K.: data curation, writing—review and editing. J.P.: data analysis, investigation. All authors have read and agreed to the published version of the manuscript.

**Funding:** The project was supported by the Ministry of Education, Youth and Sports of the Czech Republic (FRC RO70200003025/2102).

**Institutional Review Board Statement:** Not applicable.

**Informed Consent Statement:** Not applicable.

**Data Availability Statement:** Not applicable.

**Conflicts of Interest:** The authors declare no conflict of interest.

## References

1. Stejskal, J. Recent Advances in the Removal of Organic Dyes from Aqueous Media with Conducting Polymers, Polyaniline and Polypyrrole, and Their Composites. *Polymers* **2022**, *14*, 4243. [[CrossRef](#)] [[PubMed](#)]
2. Moučka, R.; Sedláček, M.; Prokeš, J.; Kasparyan, H.; Valtera, S.; Kopecný, D. Electromagnetic interference shielding of polypyrrole nanostructures. *Synth. Met.* **2020**, *269*, 116573. [[CrossRef](#)]
3. Deshpande, P.P.; Jadhav, N.G.; Gelling, V.J.; Sazou, D. Conducting polymers for corrosion protection: A review. *J. Coat. Technol. Res.* **2014**, *11*, 473–494. [[CrossRef](#)]
4. Lee, J.Y.; Park, D.W.; Lim, J.O. Polypyrrole-coated woven fabric as a flexible surface-heating element. *Macromol. Res.* **2003**, *11*, 481–487. [[CrossRef](#)]
5. Ul Hoque, M.I.; Holze, R. Intrinsically Conducting Polymer Composites as Active Masses in Supercapacitors. *Polymers* **2023**, *15*, 730. [[CrossRef](#)]
6. Ngwabebhoh, F.A.; Sába, T.; Stejskal, J.; Trchová, M.; Kopecný, D.; Pflieger, J. Conducting polypyrrole-coated leathers. *Prog. Org. Coat.* **2023**, *179*, 107495. [[CrossRef](#)]
7. Maráková, N.; Humpolíček, P.; Kašpárková, V.; Capáková, Z.; Martinková, L.; Bober, P.; Trchová, M.; Stejskal, J. Antimicrobial activity and cytotoxicity of cotton fabric coated with conducting polymers, polyaniline or polypyrrole, and with deposited silver nanoparticles. *Appl. Surf. Sci.* **2017**, *396*, 169–176. [[CrossRef](#)]
8. da Silva, F.A.G., Jr.; Vieira, S.A.; Botton, S.D.A.; da Costa, M.M.; de Oliveira, H.P. Antibacterial activity of polypyrrole-based nanocomposites: A mini-review. *Polim. Cienc. Technol.* **2020**, *30*, e2020048. [[CrossRef](#)]
9. Du, H.; Parit, M.; Liu, K.; Zhang, M.; Jiang, Z.; Huang, T.-S.; Zhang, X.; Si, C. Multifunctional Cellulose Nanopaper with Superior Water-Resistant, Conductive, and Antibacterial Properties Functionalized with Chitosan and Polypyrrole. *ACS Appl. Mater. Interfaces* **2021**, *13*, 32115–32125. [[CrossRef](#)]
10. Ngwabebhoh, F.A.; Zandrea, O.; Sába, T.; Stejskal, J.; Trchová, M.; Kopecný, D.; Pflieger, J.; Prokeš, J. In-situ coating of leather with conducting polyaniline in colloidal dispersion mode. *Synth. Met.* **2022**, *291*, 117191. [[CrossRef](#)]
11. Stejskal, J.; Prokeš, J. Conductivity and morphology of polyaniline and polypyrrole prepared in the presence of organic dyes. *Synth. Met.* **2020**, *264*, 116373. [[CrossRef](#)]
12. Stejskal, J.; Sapurina, I.; Trchová, M. Polyaniline nanostructures and the role of aniline oligomers in their formation. *Prog. Polym. Sci.* **2010**, *35*, 1420–1481. [[CrossRef](#)]

13. Beygisangchin, M.; Abdul Rashid, S.; Shafie, S.; Sadrollhosseini, A.; Lim, H. Preparations, Properties, and Applications of Polyaniline and Polyaniline Thin Films—A Review. *Polymers* **2021**, *13*, 2003. [[CrossRef](#)]
14. Balabanova, M.; Popova, L.; Tchipeva, R. Dyes in dermatology. *Clin. Dermatol.* **2003**, *21*, 2–6. [[CrossRef](#)]
15. Page, K.; Correia, A.; Wilson, M.; Allan, E.; Parkin, I. Light-activated antibacterial screen protectors for mobile telephones and tablet computers. *J. Photochem. Photobiol. A Chem.* **2015**, *296*, 19–24. [[CrossRef](#)]
16. Liang, J.-Y.; Yuann, J.-M.P.; Hsie, Z.-J.; Huang, S.-T.; Chen, C.-C. Blue light induced free radicals from riboflavin in degradation of crystal violet by microbial viability evaluation. *J. Photochem. Photobiol. B Biol.* **2017**, *174*, 355–363. [[CrossRef](#)]
17. Zhang, Y.; Yan, J.; Avellan, A.; Gao, X.; Matyjaszewski, K.; Tilton, R.D.; Lowry, G.V. Temperature- and pH-Responsive Star Polymers as Nanocarriers with Potential for *in Vivo* Agrochemical Delivery. *ACS Nano* **2020**, *14*, 10954–10965. [[CrossRef](#)]
18. Nisnevitch, M.; Nakonechny, F.; Nitzan, Y. Photodynamic antimicrobial chemotherapy by liposome-encapsulated water-soluble photosensitizers. *Russ. J. Bioorg. Chem.* **2010**, *36*, 363–369. [[CrossRef](#)]
19. Baruah, R.; Yadav, A.; Das, A.M. Evaluation of the multifunctional activity of silver bionanocomposites in environmental remediation and inhibition of the growth of multidrug-resistant pathogens. *New J. Chem.* **2022**, *46*, 10128–10153. [[CrossRef](#)]
20. de Almeida, Y.; Bispo, D.; Montalvão, M.; Mota, K.; Corrêa, C.; Gimenez, I. Effect of Preparation Additives on the Antimicrobial Activity and Cytotoxicity of Polypyrrole. *J. Braz. Chem. Soc.* **2021**, *32*, 1203–1212. [[CrossRef](#)]
21. Kaatz, G.W.; Moudgal, V.V.; Seo, S.M.; Kristiansen, J.E. Phenothiazines and Thioxanthenes Inhibit Multidrug Efflux Pump Activity in *Staphylococcus aureus*. *Antimicrob. Agents Chemother.* **2003**, *47*, 719–726. [[CrossRef](#)] [[PubMed](#)]
22. Thesnaar, L.; Bezuidenhout, J.J.; Petzer, A.; Petzer, J.P.; Cloete, T.T. Methylene blue analogues: In vitro antimicrobial minimum inhibitory concentrations and in silico pharmacophore modelling. *Eur. J. Pharm. Sci.* **2021**, *157*, 105603. [[CrossRef](#)] [[PubMed](#)]
23. Gupta, S.; Acharya, U.; Pištěková, H.; Taboubi, O.; Morávková, Z.; Kašparová, M.; Humpolíček, P.; Bober, P. Tuning the Conductivity, Morphology, and Capacitance with Enhanced Antibacterial Properties of Polypyrrole by Acriflavine Hydrochloride. *ACS Appl. Polym. Mater.* **2021**, *3*, 6063–6069. [[CrossRef](#)]
24. Wainwright, M.; Crossley, K. Methylene Blue—A Therapeutic Dye for All Seasons? *J. Chemother.* **2002**, *14*, 431–443. [[CrossRef](#)]
25. Seshadri, D.T.; Bhat, N.V. Use of polyaniline as an antimicrobial agent in textiles. *Indian J. Fibre Text. Res.* **2005**, *30*, 204–206.
26. Kuceková, Z.; Humpolíček, P.; Kašpárková, V.; Perecko, T.; Lehocký, M.; Hauerlandová, I.; Sáha, P.; Stejskal, J. Colloidal polyaniline dispersions: Antibacterial activity, cytotoxicity and neutrophil oxidative burst. *Colloids Surf. B Biointerfaces* **2014**, *116*, 411–417. [[CrossRef](#)]
27. Falak, S.; Shin, B.K.; Huh, D.S. Antibacterial Activity of Polyaniline Coated in the Patterned Film Depending on the Surface Morphology and Acidic Dopant. *Nanomaterials* **2022**, *12*, 1085. [[CrossRef](#)]
28. Varesano, A.; Vineis, C.; Aluigi, A.; Rombaldoni, F.; Tonetti, C.; Mazzuchetti, G. Antibacterial efficacy of polypyrrole in textile applications. *Fibers Polym.* **2013**, *14*, 36–42. [[CrossRef](#)]
29. Stejskal, J. Interaction of conducting polymers, polyaniline and polypyrrole, with organic dyes: Polymer morphology control, dye adsorption and photocatalytic decomposition. *Chem. Pap.* **2020**, *74*, 1–54. [[CrossRef](#)]
30. Stejskal, J.; Pekárek, M.; Trchová, M.; Kolská, Z. Adsorption of organic dyes on macroporous melamine sponge incorporating conducting polypyrrole nanotubes. *J. Appl. Polym. Sci.* **2022**, *139*, 52156. [[CrossRef](#)]
31. Stejskal, J.; Trchová, M. Conducting polypyrrole nanotubes: A review. *Chem. Pap.* **2018**, *72*, 1563–1595. [[CrossRef](#)]
32. Stejskal, J.; Trchová, M.; Bober, P.; Morávková, Z.; Kopecký, D.; Vřřata, M.; Prokeš, J.; Varga, M.; Watzlová, E. Polypyrrole salts and bases: Superior conductivity of nanotubes and their stability towards the loss of conductivity by deprotonation. *RSC Adv.* **2016**, *6*, 88382–88391. [[CrossRef](#)]
33. Stejskal, J.; Kopecký, D.; Kasparyan, H.; Vilčáková, J.; Prokeš, J.; Křivka, I. Melamine Sponges Decorated with Polypyrrole Nanotubes as Macroporous Conducting Pressure Sensors. *ACS Appl. Nano Mater.* **2021**, *4*, 7513–7519. [[CrossRef](#)]
34. Stejskal, J.; Trchová, M.; Kasparyan, H.; Kopecký, D.; Kolská, Z.; Prokeš, J.; Křivka, I.; Vajd'ák, J.; Humpolíček, P. Pressure-Sensitive Conducting and Antibacterial Materials Obtained by *in Situ* Dispersion Coating of Macroporous Melamine Sponges with Polypyrrole. *ACS Omega* **2021**, *6*, 20895–20901. [[CrossRef](#)]
35. Ungureanu, C.; Pirvu, C.; Mindroiu, M.; Demetrescu, I. Antibacterial polymeric coating based on polypyrrole and polyethylene glycol on a new alloy TiAlZr. *Prog. Org. Coat.* **2012**, *75*, 349–355. [[CrossRef](#)]
36. Mindroiu, M.; Ungureanu, C.; Ion, R.; Pirvu, C. The effect of deposition electrolyte on polypyrrole surface interaction with biological environment. *Appl. Surf. Sci.* **2013**, *276*, 401–410. [[CrossRef](#)]
37. Cabuk, M.; Alan, Y.; Yavuz, M.; Unal, H.I. Synthesis, characterization and antimicrobial activity of biodegradable conducting polypyrrole-graft-chitosan copolymer. *Appl. Surf. Sci.* **2014**, *318*, 168–175. [[CrossRef](#)]
38. da Silva, F.A.G.; Queiroz, J.C.; Macedo, E.R.; Fernandes, A.W.C.; Freire, N.B.; da Costa, M.M.; de Oliveira, H.P. Antibacterial behavior of polypyrrole: The influence of morphology and additives incorporation. *Mater. Sci. Eng. C* **2016**, *62*, 317–322. [[CrossRef](#)]
39. Balouiri, M.; Sadiki, M.; Ibsouda, S.K. Methods for in vitro evaluating antimicrobial activity: A review. *J. Pharm. Anal.* **2015**, *6*, 71–79. [[CrossRef](#)]

40. Salehi, M.H.; Golbaten-Mofrad, H.; Jafari, S.H.; Goodarzi, V.; Entezari, M.; Hashemi, M.; Zamanlui, S. Electrically conductive biocompatible composite aerogel based on nanofibrillated template of bacterial cellulose/polyaniline/nano-clay. *Int. J. Biol. Macromol.* **2021**, *173*, 467–480. [[CrossRef](#)]
41. Carvalho, I.; Ferdov, S.; Mansilla, C.; Marques, S.; Cerqueira, M.; Pastrana, L.; Henriques, M.; Gaidau, C.; Ferreira, P.; Carvalho, S. Development of antimicrobial leather modified with Ag–TiO<sub>2</sub> nanoparticles for footwear industry. *Sci. Technol. Mater.* **2018**, *30*, 60–68. [[CrossRef](#)]
42. Kopecký, D.; Varga, M.; Prokeš, J.; Vrnata, M.; Trchová, M.; Kopecká, J.; Václavík, M. Optimization routes for high electrical conductivity of polypyrrole nanotubes prepared in presence of methyl orange. *Synth. Met.* **2017**, *230*, 89–96. [[CrossRef](#)]

**Disclaimer/Publisher's Note:** The statements, opinions and data contained in all publications are solely those of the individual author(s) and contributor(s) and not of MDPI and/or the editor(s). MDPI and/or the editor(s) disclaim responsibility for any injury to people or property resulting from any ideas, methods, instructions or products referred to in the content.